A mechanical realisation of a symplectic numerical method with large step-size

S.C. Green, C.J. Budd and G.W. Hunt
Centre for Nonlinear Mechanics, University of Bath, Bath
BA2 7AY
cjb@maths.bath.ac.uk

Abstract

We show that a mechanical model of a pin-jointed linked structure is exactly equivalent to a symplectic Euler discretisation of a Hamiltonian ODE system. The step-size of this discretisation relates to a mechanical quantity which can take arbitrary values. Thus we may explore the behaviour of the symplectic Euler method in regions not normally considered appropriate for a numerical scheme and investigate the use of backward error analysis in describing the behaviour of the pin-jointed structure.

1 Introduction

We have become very familiar with the process of taking a system of Hamiltonian differential equations, discretising this by using a symplectic method with step size h and then studying the dynamics of the resulting discrete system. As the resulting system leads to a symplectic map we may analyse it by using the theory of such maps, including KAM theory. We can also, of course, use backward error analysis [12] to relate the behaviour of the discrete system to that of the underlying continuous system provided that the step-size h is sufficiently small.

However, we should realise that many discrete, symplectic, systems arise not from discretisations of differential equations, but directly from physical and other applications. Any problem involving lattices, cells or composite materials is naturally discrete. A 'traditional' approach to studying such systems has often been to ignore their discrete nature, treat them as continuous problems described by differential equations, and to then discretise the resulting equations. This process can be somewhat perverse, and indeed may not even be appropriate if the natural length scale of the original discrete system is relatively large. Indeed it may often be much simpler to work directly with the original discrete system and bypass the continuum approximation. Such is the power of the geometric integration approach that it may well be possible to analyse this discrete system directly using geometric

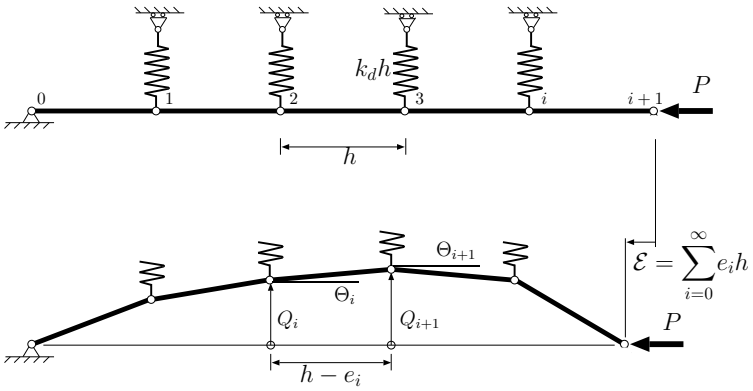

Figure 1: The discrete system of linked rods in a flat state (top) and displaced state (bottom). Adapted from [8].

integration techniques, even though it is not derived directly as a numerical discretisation. Thus geometric integration can be seen as a powerful analytic tool which extends beyond numerical analysis!

In this paper we will demonstrate the effectiveness of this approach by looking at the equilibrium states of a naturally occurring mechanical system illustrated in Figure 1. This comprises a semi-infinite series of finite length links, joined by frictionless pins, supported by elastic springs and compressed horizontally by an axial load P. The equilibrium state, described in terms of the vertical displacement Q_i and Θ_i the angle of the ith link, satisfies a second order *difference* equation. If the length h of each of the links is small and if the difference between the angle of inclination of adjacent links links is also small we may approximate such a system by a second order (in space) nonlinear Hamiltonian differential equation $N(q)$ (which we can then discretise). Note, that in common with many such mechanical systems [7, 9, 10, 11] we think of the spatial variable x as playing the role usually taken by time t. As there is no preferred spatial direction and position, such mechanical systems usually have reflectional symmetry ($x \to -x$) and translational symmetry and are thus often described by reversible Hamiltonian equations. Thus they are a very natural set of examples to which symplectic methods can be applied and it is somewhat surprising that they have not been looked at more often in the geometric integration literature.

The approximation of the displacement of the linked structure by the solution of a differential equation ceases to be a good one when either h and/or the difference of angle of adjacent links increases. We will show, however, that the equilibrium state can still be described in terms of a *symplectic map* ϕ between $(Q_i, W_i \equiv -\tan(\Theta_{i-1}))$ and (Q_{i+1}, W_{i+1}). It

is then natural to ask what form the behaviour of the iterates of ϕ takes. Observe that in the mechanical system this question is valid for all values of h but to address it we first consider the case of h small. We will show that in this case the map ϕ is *exactly the same* as a discretisation of the differential equation $N(q)$ using a *Symplectic Euler-B Method*. We can thus study the iterates of ϕ using backward error analysis [12], [5]. Remarkably, the discrete system obtained from the Symplectic Euler-B discretisation of $N(q)$ continues to exactly describe the underlying discrete physical system even for large values of h. We show that this follows naturally from a consideration of the discrete Lagrangian of the mechanical system and applying the theory of Marsden and West [13].

Thus, it is quite legitimate, to consider the study of this discrete system for values of h which would normally be considered inappropriate for a numerical discretisation of the differential equation $N(q)$. The resulting system then exhibits interesting periodic and chaotic behaviour, with break up of tori as h increases.

The layout of the remainder of this paper is as follows. In Section 2 we describe the discrete model for the mechanical system and show that by choosing coordinates correctly it can be described in terms of the symplectic map ϕ. In Section 3 we derive the continuous system $N(q)$ which arises in the limit of small h and examine its various properties. In Section 4 we show the equivalence of the Euler-B discretisation of N and the original discrete system and apply backward error analysis to analyse the iterates of ϕ. Finally in section 5 we look at the large h limit of the dynamics.

2 The mechanical discrete system

The discrete mechanical system described here, and shown in Figure 1, has been studied before [8] in the context of spatial chaos. The first part of this section reproduces some of the analysis in [8], with slightly different notation, to show how the equilibrium states of the system are described by a pair of coupled first order difference equations.

This system comprises a set of links of length h for which the rotation of each link from the horizontal in an anticlockwise direction (Figure 1) is Θ_i. The end shortening due to an individual link e_i (i.e. the difference

in the horizontal displacement of its end points) is

$$e_i = \begin{cases} h\left(1 - \sqrt{1 - \left(\frac{Q_{i+1}-Q_i}{h}\right)^2}\right) & \text{for} \quad -\pi/2 \le \Theta_i \le \pi/2 \\ h\left(1 + \sqrt{1 - \left(\frac{Q_{i+1}-Q_i}{h}\right)^2}\right) & \text{for} \quad \pi/2 \le |\Theta_i| \le \pi \end{cases},$$

we shall consider only the first of these two θ_i ranges. With U denoting the total potential energy of the springs (linear with their stiffness $k = k_d h$ written in terms of the stiffness per unit length k_d) and $P\mathcal{E}$ denoting the work done by the load P in compressing the system by a horizontal amount $\mathcal{E} = \sum e_i$ the total potential energy of the system is

$$E = U - P\mathcal{E} = \tfrac{1}{2} k_d h \sum_{i=0}^{\infty} Q_i^2 - Ph \sum_{i=0}^{\infty} \left(1 - \sqrt{1 - \left(\frac{V_i}{h}\right)^2}\right), \quad (1)$$

where $V_i = Q_{i+1} - Q_i$.

The equilibrium configuration for this system is given when $\frac{\partial E}{\partial Q_i} = 0 \; \forall \; i$. Differentiating (1) with respect to the coordinate Q_i gives, after some manipulation, the second order difference equation

$$Q_i + \frac{P}{k_d h}\left(\frac{\frac{V_i}{h}}{\sqrt{1 - \left(\frac{V_i}{h}\right)^2}} - \frac{\frac{V_{i-1}}{h}}{\sqrt{1 - \left(\frac{V_{i-1}}{h}\right)^2}}\right) = 0. \quad (2)$$

This can be re-written as a pair of coupled first order difference equations

$$Q_{i+1} = Q_i + V_i \quad (3)$$

$$\frac{V_{i+1}}{h} = \frac{\beta_i}{\sqrt{1 + \beta_i^2}} \quad (4)$$

where

$$\beta_i = \frac{\frac{V_i}{h}}{\sqrt{1 - \left(\frac{V_i}{h}\right)^2}} - \frac{k_d h}{P} Q_{i+1}.$$

We will treat this coupled set of first order equations as an initial value problem on the semi-infinite domain $i \in \mathbb{N} \cup \{0\}$ with Q_0, V_0 specified.

2.1 A symplectic choice of coordinates

We now demonstrate that the nonlinear map described in (3) and (4) is symplectic when expressed in an appropriate coordinate system. To do

this we transform the coordinate V_i using

$$W_{i+1} = \frac{\frac{-V_i}{h}}{\sqrt{1-\left(\frac{V_i}{h}\right)^2}} \equiv -\tan\Theta_i$$

and leave the Q_i coordinate unchanged. Performing this change in equations (3) and (4) gives

$$Q_{i+1} = Q_i - \frac{hW_{i+1}}{\sqrt{1+W_{i+1}^2}}, \qquad W_{i+1} = W_i + \frac{k_d h}{P} Q_i$$

or equivalently a map $\phi : \mathbb{R}^2 \to \mathbb{R}^2$ defined by

$$\phi : \quad \begin{pmatrix} Q_i \\ W_i \end{pmatrix} \mapsto \begin{pmatrix} Q_i - \frac{h\left(W_i + \frac{k_d h}{P} Q_i\right)}{\sqrt{1+\left(W_i + \frac{k_d h}{P} Q_i\right)^2}} \\ W_i + \frac{k_d h}{P} Q_i \end{pmatrix}. \tag{5}$$

This map has Jacobian $\psi_{ij} = \frac{\partial \phi_i}{\partial x_j}$ given by

$$\psi = \begin{pmatrix} 1 - \frac{k_d h^2}{P\left(1+\left(W_i + \frac{k_d h}{P} Q_i\right)^2\right)^{\frac{3}{2}}} & \frac{-h}{\left(1+\left(W_i + \frac{k_d h}{P} Q_i\right)^2\right)^{\frac{3}{2}}} \\ \frac{k_d h}{P} & 1 \end{pmatrix}$$

Performing the matrix multiplication $\psi^T J^{-1} \psi$ verifies that the map ϕ satisfies the symplecticness condition

$$\psi^T J^{-1} \psi = J^{-1}, \tag{6}$$

where $J^{-1} = \begin{pmatrix} 0 & -1 \\ 1 & 0 \end{pmatrix}$ is the inverse structure matrix.

2.2 Nondimensionalisation

We can nondimensionalise ϕ by letting

$$\alpha = \frac{P}{k_d}, \quad Q_i = \sqrt{\alpha} U_i \text{ and } h = \sqrt{\alpha}\Delta t.$$

This leads to the nondimensional map

$$\Phi : \quad \begin{pmatrix} U_i \\ W_i \end{pmatrix} \mapsto \begin{pmatrix} U_i - \Delta t \frac{W_i + \Delta t U_i}{\sqrt{1+(W_i+\Delta t U_i)^2}} \\ W_i + \Delta t U_i \end{pmatrix}. \tag{7}$$

Note that for a physical system with unit spring constant per unit length k_d and unit compressive load P, ϕ and Φ are equivalent when h is numerically equal to Δt.

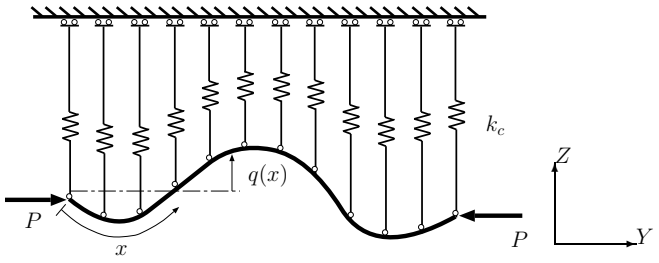

Figure 2: The continuous strut under consideration, with zero bending stiffness on a foundation of spring constant per unit length k_c.

3 The continuous strut equation

We now seek a continuous system which has equilibrium states that approximate the equilibrium states of the discrete system described in the previous section. So consider the system that would results from letting $h \to 0$ in Figure 1. This system is shown in Figure 2 and on physical grounds we introduce the continuous strut which will be analysed, initially, in a similar way to the discrete case of section 2.

Figure 2 shows a semi-infinite strut with no bending stiffness, supported on a linear elastic foundation of spring constant per unit length k_c. The deflection of the strut q is a function of the coordinate x which varies along the length of the strut and there is an applied axial load P. As in the discrete case we write the total potential energy of the system as the energy stored in the foundation minus the work done by the applied load: $E = U - P\mathcal{E}$,

$$E = \tfrac{1}{2}k_c \int_0^\infty q^2 \, \mathrm{d}x - P \int_0^\infty \left(1 - \sqrt{1 - q'^2}\right) \, \mathrm{d}x. \tag{8}$$

This expression contains the implicit gradient restriction $-1 < q' < 1$. Seeking stationary solutions $q(x)$ of the total potential energy (8) is equivalent to finding stationary solutions of the functional

$$\bar{E} = \int_0^\infty \left(\tfrac{1}{2}k_c q^2 + P\sqrt{1 - q'^2}\right) \mathrm{d}x.$$

The Euler-Lagrange equation $\frac{\delta E}{\delta q}$ leads to the differential equation

$$N(q) \equiv q'' + \frac{k_c}{P} q (1 - q'^2)^{\frac{3}{2}} = 0. \tag{9}$$

As with the difference equation of section 2 we will treat this as an initial value problem on the domain $x \in \mathbb{R}^+ \cup \{0\}$. Some properties of this differential equation are now presented.

3.1 Nondimensionalisation

If in the differential equation (9) we make the following changes of variable

$$\alpha = \frac{P}{k}, \quad q = \sqrt{\alpha}u \quad \text{and} \quad x = \sqrt{\alpha}t \tag{10}$$

the equation becomes independent of the parameter α and has the nondimensional form

$$N(u) \equiv \ddot{u} + u(1 - \dot{u}^2)^{\frac{3}{2}} = 0 \tag{11}$$

where $\dot{u} = \frac{\mathrm{d}u}{\mathrm{d}t}$.

This non-dimensionalisation is a scale transform of the physical (y, z) plane with scale factor $\alpha^{-\frac{1}{2}}$.

3.2 Hamiltonian form

The differential equation (11) can be written in canonical Hamiltonian form. Motivated by the choice of coordinates in section 2.1, we choose the generalised coordinates to be

$$u \qquad \text{and} \qquad w = \frac{-\dot{u}}{\sqrt{1 - \dot{u}^2}}. \tag{12}$$

The Hamiltonian is then given by

$$H_0 = -\sqrt{1 + w^2} - \frac{u^2}{2}. \tag{13}$$

The differential equation $N(u)$ is recovered by substituting the transformations (12) into Hamilton's equations applied to (13). Note that H_0 is separable and translation invariant. The Hamiltonian (13) is also even with respect to the momentum coordinate w and so this continuous system is time reversible.

3.3 Analytic Solution

The differential equation $N(u)$ has a closed form solution. As H is translation independent it is conserved along trajectories and so if the Hamiltonian function for a particular trajectory has value $-E_H$ we can substitute (12) into (13) to give

$$E_H = \frac{1}{1 - \dot{u}^2} + \frac{u^2}{2}$$

so that

$$\frac{\mathrm{d}u}{\mathrm{d}t} = \sqrt{1 - \left(E_H - \frac{u^2}{2}\right)^{-2}}.$$

This can be integrated to give an analytic solution in terms of the incomplete elliptic integrals of the first and second kinds:

$$t+t_0 = \sqrt{\frac{2}{E_H+1}}\left[(E_H+1)\int_0^{\gamma v}\frac{\sqrt{1-k^2\theta^2}}{\sqrt{1-\theta^2}}\,\mathrm{d}\theta - \int_0^{\gamma v}\frac{\mathrm{d}\theta}{\sqrt{1-\theta^2}\sqrt{1-k^2\theta^2}}\right] \tag{14}$$

where $k = \sqrt{\frac{E_H-1}{E_H+1}}$ is the elliptic modulus, $\gamma = [2(E_H-1)]^{-1/2}$ and t_0 is an arbitrary constant.

4 The link between the continuous and discrete systems

In this section we show that the symplectic mapping Φ is equivalent to the symplectic Euler-B discretisation of the Hamiltonian differential equation $N(u)$ with Hamiltonian (13). For a separable Hamiltonian system ($H = T(w)+V(u)$) the symplectic Euler-B discretisation is given by

$$\begin{aligned} U_{i+1} &= U_i + \Delta t \left.\frac{\mathrm{d}T}{\mathrm{d}w}\right|_{W_{i+1}} \\ W_{i+1} &= W_i - \Delta t \left.\frac{\mathrm{d}V}{\mathrm{d}u}\right|_{U_i} \end{aligned}$$

Applying this discretisation to the system with Hamiltonian (13) gives

$$U_{i+1} = U_i - \Delta t \frac{W_{i+1}}{\sqrt{1+W_{i+1}^2}}, \quad W_{i+1} = W_i + \Delta t\, U_i$$

which defines a mapping identical to the discrete mapping Φ from equation (7). Note that while this mapping only numerically approximates $N(u)$ for small Δt it describes the equilibrium configurations of the pin jointed mechanical structure for all values of Δt. This surprising result can be explained by the theory of variational integration reviewed by Marsden and West in [13].

4.1 Variational integration

Variational integration is an effective way of deriving symplectic numerical integration schemes for differential equations that have a variational formulation. In this section we briefly describe how the theory from [13] helps to explain the link between the discrete mechanical system and the Euler-B integration algorithm.

To derive a variational integrator for a system described by a Lagrangian $L(u, \dot{u})$ with action $S = \int L(u(t), \dot{u}(t))\,\mathrm{d}t$ we must form an approximation, $L_d(U_i, U_{i+1})$, of the exact discrete Lagrangian

$$L_d^E(U_i, U_{i+1}) = \int_{t_i}^{t_{i+1}} L(u(t), \dot{u}(t))\,\mathrm{d}t, \tag{15}$$

where $u(t_i) = U_i$ and $u(t_{i+1}) = U_{i+1}$, using a simple quadrature scheme. The discrete action then becomes $S_d = \sum_i L_d(U_i, U_{i+1})$; requiring this action to be stationary with respect to the U_i then leads to discrete analogs of the Euler-Lagrange equations, the Legendre transform and the associated Hamiltonian flow map. It is this discrete Hamiltonian flow map that integrates the differential equation that results from applying the standard Euler-Lagrange equations to the continuous Lagrangian $L(u, \dot{u})$.

The difference equation (2) was derived by requiring the energy E to be stationary with respect to the U_i, it is also autonomous and so we can rescale E by a multiplicative factor and add constants without changing the difference equation (2). Using these facts we can nondimensionalise E and rewrite it as

$$\begin{aligned} E &= \sum_{i=0}^{\infty} L_d^{(1)}(U_i, U_{i+1}) \\ L_d^{(1)}(U_i, U_{i+1}) &= \tfrac{1}{2}\Delta t U_i^2 + \Delta t\sqrt{1 - \left(\frac{U_{i+1} - U_i}{\Delta t}\right)^2}. \end{aligned} \tag{16}$$

This expression is a simple approximation of the exact discrete Lagrangian for the differential equation $N(u)$:

$$\begin{aligned} L_d^E = \int_{t_i}^{t_{i+1}} &\left(\tfrac{1}{2}u(t)^2 + \sqrt{1 - \dot{u}(t)^2}\right)\,\mathrm{d}t \\ &u(t_i) = U_i \quad u(t_{i+1}) = U_{i+1} \end{aligned}$$

using a forward finite difference gradient approximation and the rectangle quadrature rule. This particular approximation leads to the symplectic Euler-B numerical integrator and its discrete Hamiltonian flow map is exactly the map Φ.

Note that if considered the other half space $i = 0, -1, -2, \ldots, -\infty$ we could rewrite E in the subtly different form

$$E = \sum_{i=-1}^{-\infty} L_d^{(2)}(U_i, U_{i+1})$$

$$L_d^{(2)}(U_i, U_{i+1}) = \tfrac{1}{2}\Delta t U_{i+1}^2 + \Delta t\sqrt{1 - \left(\frac{U_{i+1} - U_i}{h}\right)^2},$$

the differences being the subscript of the U_{i+1}^2 term and the limits of the sum. This is the adjoint of the discrete Lagrangian (16) (i.e. $L_d^{(1)}(U_i, U_{i+1}, \Delta t) = -L_d^{(2)}(U_{i+1}, U_i, -\Delta t)$) and so as proved in [13] the discrete Hamiltonian flow map resulting from $L_d^{(2)}$ is the adjoint of the Euler-B method that results from $L_d^{(1)}$: the Euler-A integrator

$$\begin{aligned} U_{i+1} &= U_i + \Delta t \left.\frac{\mathrm{d}T}{\mathrm{d}w}\right|_{W_i} \\ W_{i+1} &= W_i - \Delta t \left.\frac{\mathrm{d}V}{\mathrm{d}u}\right|_{U_{i+1}}. \end{aligned}$$

This suggests that the discretisation that exactly describes the discrete physical system depends on the spatial direction we are interested in (i.e. $i \to +\infty$ or $i \to -\infty$). Further analysis in this direction will be left for future work and so in the remainder of this paper we will continue to consider the Euler-B discretisation with the variables $i \in \mathbb{N} \cup \{0\}$ and compare it with the differential equation $N(u)$ on the domain $x \in \mathbb{R}^+ \cup \{0\}$.

4.2 The modified equation

We now have one parameter Δt, the numerical step size, that tells us how closely or otherwise the solutions to the discrete system approximate the continuous one. Using backward error analysis it is possible to derive a continuous Hamiltonian that the discrete system solves almost exactly when Δt is small. The book by Leimkuhler and Reich [12] gives an expression for the modified Hamiltonian of the Euler-B discretisation of a separable system ($H = T(w) + V(u)$) in the form

$$H_{\Delta t} = T + V - \frac{\Delta t}{2}\{V, T\} + \frac{\Delta t^2}{12}\left(\{V, \{V, T\}\} + \{T, \{T, V\}\}\right) + \ldots \quad (17)$$

where $\{\ldots, \ldots\}$ denotes the canonical Lie-Poisson bracket. Evaluating the first two terms in this expression for the Hamiltonian (13) gives

$$H_{\Delta t} = -\sqrt{1 + w^2} - \frac{u^2}{2} - \Delta t \frac{u}{2}\frac{w}{\sqrt{1 + w^2}} + \mathcal{O}(\Delta t^2). \quad (18)$$

The asymptotic expansion (17) does not converge; however it has been shown [14] that if the series is truncated after a certain number of terms $i_*(\Delta t, \gamma, c)$ for some $\gamma, c > 0$ that $|\tilde{\Phi}_{\Delta t}(u_0, w_0) - \Phi(u_0, w_0)| \leq 3c\Delta t \mathrm{e}^{-\gamma/\Delta t}$ where $\tilde{\Phi}$ represents the flow of (17) and Φ is the Euler-B discretisation of (11). (I.e. the flow of the optimally truncated part of $H_{\Delta t}$ and the iterates of Φ agree up to terms exponentially small in Δt.)

The above analysis holds for $0 \leq \Delta t < \delta$ for some small $\delta(c, \gamma)$. We wish to investigate how high Δt can be taken while the flow of a finite truncation of $H_{\Delta t}$ shows some agreement with the iterates of Φ. To do this we will truncate the above series to $\mathcal{O}(\Delta t)$ and study the dynamics of the system described by the following Hamiltonian

$$H_1 = H_0 - \Delta t \frac{u}{2} \frac{w}{\sqrt{1 + w^2}}. \tag{19}$$

Figure 5 shows the level sets of the Hamiltonian H_0 (13), which do not depend on Δt, for comparison with other figures.

5 The behaviour of the system for large Δt

In this section we will compare the iterates of Φ, which exactly describe the original discrete system, with the dynamics of the truncated modified system with Hamiltonian H_1 as Δt increases.

We shall start at the continuum limit. Since Φ is a first order symplectic Euler discretisation of the continuous system $N(u)$ (13) we know that over a finite time interval $|\Phi(u_0, w_0) - \hat{\Phi}_{\Delta t}(u_0, w_0)| \leq C\Delta t^2$, where $\hat{\Phi}$ denotes the flow of $N(u)$.

Away from the continuum limit the backward error analysis of section 4.2 gives us a modified Hamiltonian (17) the flow map of which ($\tilde{\Phi}$) is integrated by Φ almost exactly: up to terms exponentially small in Δt. This tells us for times that are not exponentially long the iterates of Φ will lie on the contour of (17) that corresponds to the same initial conditions. These contours form a one parameter family of periodic orbits parametrised by the, conserved, value of the modified Hamiltonian (Figure 3 (d)). This in turn is approximated to $\mathcal{O}(\Delta t^2)$ but the Hamiltonian system H_1.

In Figure (3) we compare the orbits of Φ (in (a),(b) & (c)) with the level sets of H_1 for differing values of Δt. As might be expected the agreement is good for Δt small (e.g. $\Delta t = 0.05$) and less good for larger Δt. However, even for larger Δt, if we look close to the origin there is surprisingly good agreement between the iterates of Φ and the truncated

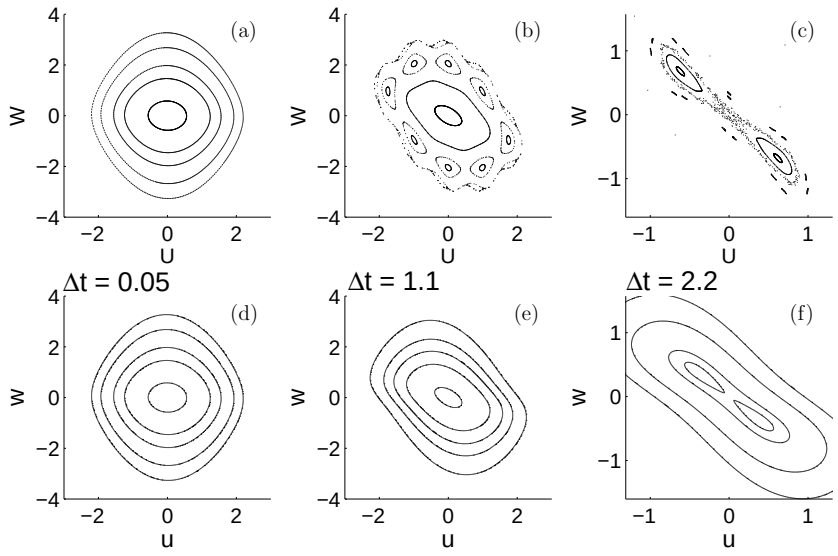

Figure 3: Phase portraits for the iterates of the map Φ (top row) and the level sets of the truncated modified Hamiltonian H_1 (19) (bottom row) for $\Delta t = 0.05, 1.1, 2.2$.

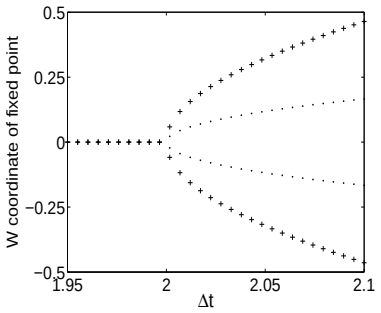

Figure 4: Momentum coordinate w of the secondary fixed points that are generated by the bifurcation at $\Delta t = 2$. The crosses indicate the position of the period fixed point of the map Φ and the dots show the two stable fixed points of the truncated modified Hamiltonian H_1.

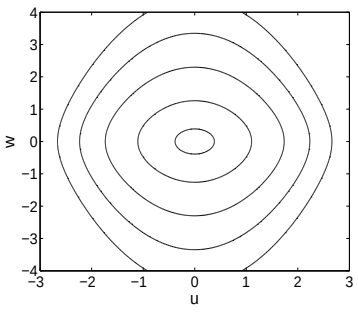

Figure 5: Level sets of the Hamiltonian H_0 (13), which are independent of Δt.

modified Hamiltonian H_1. The map Φ has a fixed point at the origin with linearisation

$$\begin{pmatrix} u \\ w \end{pmatrix} \to \mathrm{A} \begin{pmatrix} u \\ w \end{pmatrix} \text{ where } \mathrm{A} = \begin{pmatrix} 1-\Delta t^2 & -\Delta t \\ \Delta t & 1 \end{pmatrix}.$$

This fixed point is stable (Fig. 3 (a) & (b)) if $\Delta t < 2$ and loses stability when $\Delta t = 2$ at which point A has an eigenvalue of -1. For $\Delta t > 2$ there is an unstable saddle, a period two fixed point (Figure 3 (c)) and a homoclinic orbit from the origin to itself. This bifurcation is equivalent (but traversed the opposite direction) to the buckling of the discrete physical system described in [8] where the zero solution loses stability and is not observed in the analytic solution to the original continuous system (14). As we increase Δt through $\Delta t = 2$ we are taking the physical system from the post-buckling regime into the low load pre-buckling region. The surprising feature of the truncated modified Hamiltonian (19) is that it too exhibits a similar bifurcation from a stable fixed point (Figure 3 (d) & (e)) to a saddle, two further stable fixed points (Figure 3 (f)) and a homoclinic orbit at the same value of $\Delta t = 2$. This can be seen by linearising (19) about the origin so that

$$H_1 = 1 + \frac{u^2}{2} + \frac{w^2}{2} + \frac{uw\Delta t}{2} + \mathcal{O}(w^4) + \mathcal{O}(uw^3\Delta t)$$

$$\begin{aligned} \mathrm{D}^2 H_1 \equiv \begin{pmatrix} H_{uu} & H_{uw} \\ H_{wu} & H_{ww} \end{pmatrix} &= \begin{pmatrix} 1 & \Delta t/2 \\ \Delta t/2 & 1 \end{pmatrix} \\ |\mathrm{D}^2 H_1| = 0 \quad &\Rightarrow \quad 1 - \frac{\Delta t^2}{4} = 0 \\ \Rightarrow \quad \Delta t = 2. & \end{aligned}$$

The $\mathcal{O}(\Delta t^2)$ and $\mathcal{O}(\Delta t^3)$ terms in the expansion $H_{\Delta t}$ are respectively

$$\Delta t^2 K_2 \equiv \frac{-\Delta t^2\left(u^2 - \sqrt{1+w^2}\right)}{12(1+w^2)^{3/2}} \text{ and } \Delta t^3 K_3 \equiv \frac{-\Delta t^3 uw}{12(1+w^2)^2}.$$

Interestingly if we truncate $H_{\Delta t}$ by considering the system with Hamiltonian $H_2 = H_1 + \Delta t^2 K_2$ then the bifurcation at the origin does not occur when $\Delta t = 2$; however the system with Hamiltonian $H_3 = H_1 + \Delta t^2 K_2 + \Delta t^3 K_3$ has again the correct bifurcation point. Investigation of the conditions under which the truncated modified Hamiltonian shares this important bifurcation with the mechanical system is left for future work.

For larger Δt and further from the origin there is a dramatic break up of the periodic orbits exhibited by the map Φ. This break up happens in a regular and distinctive fashion and starts with the high amplitude

orbits. On break up certain periodic orbits form fixed points surrounded by islands of small amplitude oscillations about these fixed points (Figure 3 (b)). As the 'layers' peel outwards the space between these islands of periodicity is filled with irregular, high amplitude iterates.

As we move beyond $\Delta t = 2$ the agreement between the modified Hamiltonian H_1 (19) and the iterates of Φ breaks down. Figure 4 shows the w coordinate of the primary fixed point ($\Delta t < 2$) and secondary fixed points ($\Delta t > 2$) for the map Φ (crosses) and truncated modified Hamiltonian(dots). This tells us that although the modified Hamiltonian does demonstrate the physically important bifurcation, once the non-linear effects become significant further from the origin the modified Hamiltonian becomes a less useful tool in analysing the iterates of Φ.

6 Conclusions

In the previous sections the discrete physical system considered in [8] is shown to be mathematically equivalent to the symplectic, Euler-B discretisation of a Hamiltonian differential equation that describes the equilibrium configuration of a strut with zero bending stiffness on a linear foundation. The numerical step size in this discretisation Δt is equivalent to a parameter of the discrete system that can take arbitrary positive values. Applying backward error analysis, a key technique in geometric integration, allowed us to derive a continuous Hamiltonian system that not only was the continuum limit of the discrete system, as with standard continuum approximations to discrete physical systems, but for small Δt agreed almost exactly with the iterates of the discrete system (up to terms exponentially small in Δt). For larger Δt and close to the origin of phase space this new continuous system showed good agreement with the discrete system up to Δt values as high as two. At $\Delta t = 2$ the discrete physical system undergoes an important bifurcation which, remarkably, was also exhibited by the modified continuous system. Further from the origin of phase space for Δt approaching order one where the agreement of the modified continuous system with the discrete map started to fail and a dramatic break up of periodic solutions to the discrete system was observed.

In practical terms, the continuum limit has carries less immediate significance than the related discrete problem. The regular periodic solutions of Fig.3 (a) and (d) make perfect sense for the initial discrete problem and also for a strut with bending stiffness. But in the absence of bending stiffness the system would be incapable of handling the bending moments involved and would respond to load by wrinkling up with zero wavelength. So, in the process of drawing towards the continuum limit it

might appear that most of the physics is lost. It is then interesting to see that backward error analysis on this continuum limit can again retrieve much of this lost information in a systematic way. As an example, the Hamiltonian of the continuous problem carries only periodic solutions, but by adding the first order Δt term the bifurcation structure of the discrete problem is then revealed (see Fig. 3(f)), with accompanying localized homoclinic solutions giving a figure-of-eight shape in phase space. However, this level of analysis does not manage to represent successfully the break-up into quasi-periodic tori seen in the original discrete mapping; here extra terms in Δt may be needed.

Of course many questions remain; for example, what is the relation between a similar discrete system, with nearest and next nearest neighbour interactions, and the differential equation that gives the equlibrium states of a strut with non-zero bending stiffness

$$u''''(x) + Pu''(x) + f(u(x)) = 0?$$

Similarly, can we say the same about PDE's which include the time dependence of the system such as

$$u''''(x,t) + Pu''(x,t) + f(u(x,t)) = \alpha\frac{\partial u(x,t)}{\partial t} + \beta\frac{\partial^2 u(x,t)}{\partial t^2}?$$

Systems which are similar to discretisations in the x dimension of the above equation are studied in connection with localised excitations on discrete lattices known as Breathers [4, 6] and also lattice differential equations [3]. So with the ideas of geometric integration, variational integration and symplectic maps, to which Arieh Iserles has generously contributed we are looking forward to further investigating the links between these separate fields.

7 Acknowledgements

This work has been supported by an EPSRC DTA Grant and EPSRC Bath Institute for Complex Systems (BICS) grant GR/S86525/01. We wish Arieh Iserles many happy returns on his 60th birthday!

References

[1] G. I. Barenblatt. *Scaling, Self-similarity, and Intermediate Asymptotics*. Cambridge University Press, Cambridge, 1996.

[2] C. J. Budd and M. Piggot. Geometric integration and its applications. *Handbook of numerical analysis*, 35:87–109, 2003.

[3] S.-N. Chow, J. Mallet-Paret, and E. S. V. Vleck. Dynamics of lattice differential equations. *Int. J. of Bifurcation and Chaos*, 6(9):1605–1621, 1996.

[4] S. Flach and C. R. Willis. Discrete breathers. *Physics Reports*, 295:181–264, 1998.

[5] E. Hairer, C. Lubich, and G. Wanner. *Geometric Numerical Integration*. Springer Series in Computational Mathematics. Springer, 2002.

[6] D. Hennig. Next-nearest neighbor interaction and localized solutions of polymer chains. *Eur. Phys. J. B*, 20:419–425, 2001.

[7] G. W. Hunt, H. M. Bolt, and J. M. Thompson. Structural localization phenomena and the dynamical phase-space analogy. *Proc. R. Soc. Lond. A*, 425:245–267, 1989.

[8] G. W. Hunt, R. Lawther, and P. Providencia E Costa. Finite element modelling of spatially chaotic structures. *International Journal for Numerical Methods in Engineering*, 40:2237–2256, 1997.

[9] G. W. Hunt, G. J. Lord, and A. R. Champneys. Homoclinic and heteroclinic orbits underlying the post-buckling of axially-compressed cylindrical shells. *Computer Methods in Applied Mechanics and Engineering*, 170:239–251, 1991.

[10] G. W. Hunt, M. A. Peletier, A. R. Champneys, P. D. Woods, M. A. Wadee, C. J. Budd, and G. Lord. Cellular buckling in long structures. *Nonlinear Dynamics*, 21:3–29, 2001.

[11] G. W. Hunt and M. K. Wadee. Comparative lagrangian formulations for localized buckling. *Proc. R. Soc. Lond. A*, 434:485–502, 1991.

[12] B. Leimkuhler and S. Reich. *Simulating Hamiltonian Dynamics*, volume 14 of *Cambridge Monographs on Applied and Computational Mathematics*. Cambridge University Press, 2004.

[13] J. E. Marsden and M. West. Discrete mechanics and variational integrators. *Acta Numerica*, pages 357–514, 2001.

[14] S. Reich. Backward error analysis for numerical integrators. *SIAM J. Numer. Anal.*, 36:475–491, 1999.